Intestinal permeability of agaro-oligosaccharides: Transport across Caco-2 cell monolayers and pharmacokinetics in rats

Ikuya Shirai[1,2], Koji Karasawa[2], Yusuke Kodaira[3], Yu Iwasaki[4], Yasutaka Shigemura[4], Hidefumi Makabe[1,3] and Shigeru Katayama[1,3]*

[1]Department of Science and Technology, Graduate School of Medicine, Science and Technology, Shinshu University, Nagano, Japan, [2]Ina Food Industry Co., Ltd., Ina, Japan, [3]Department of Biomolecular Innovation, Institute for Biomedical Sciences, Shinshu University, Nagano, Japan, [4]Faculty of Domestic Science, Tokyo Kasei University, Tokyo, Japan

Agaro-oligosaccharides (AOSs), even-numbered oligosaccharides prepared from agar, are applied to various food, including supplements, drinks, and jellies because of their biological activities. This study aimed to evaluate the AOS permeation in the gastrointestinal tract *in vivo* and *in vitro*. Agarobiose (Abi), agarotetraose (Ate), and agarohexaose (Ahe) were detected in rat plasma after oral administration of AOSs. The detection level of agarobiose in the plasma was higher than that of agarohexaose, which was consistent with the permeation study using Caco-2 cell monolayers. Further, the adenosine triphosphate inhibitor (sodium azide) or endocytosis inhibitor (colchicine) did not inhibit AOS permeation through Caco-2 cell monolayers. Conversely, AOS permeation enhanced upon treatment with cytochalasin B, a tight junction disrupter, suggesting that AOSs might have passed mainly through the tight junctions between the intestinal epithelial cells. These results indicate that AOSs, especially agarobiose, can be absorbed as an intact form *via* the gastrointestinal tract across the intestinal epithelium through the paracellular pathway.

KEYWORDS

agaro-oligosaccharide, Caco-2, intestinal permeability, paracellular pathway, agarobiose

Introduction

Agar, a linear galactan extracted from red seaweed, has been consumed in Asian countries for a long time. Agarose, a major polysaccharide in agar, consists of alternating $(1\rightarrow 3)$-linked β-D-galactose (Gal) and $(1\rightarrow 4)$-linked 3,6-anhydro-α-L-galactose (AnGal) residues (1). Two kinds of oligosaccharides can be produced from agar depending on the type of sugar at the reducing end: agaro-oligosaccharides (AOSs) or

neoagaro-oligosaccharides. Under mildly acidic conditions, the α-(1→ 3)-galactosidic bond of agarose is hydrolyzed to AOSs composed of repeating agarobiose (Abi) units with AnGal at the reducing end (2).

Agaro-oligosaccharides have attracted considerable attention in the food, cosmetic, and pharmaceutical industries because of their biological effects, including antioxidant (3, 4), anti-inflammatory (5), anti-tumor (6), and anti-obesity (7) activities. Regarding their effects on intestinal function, several studies have demonstrated that orally administered AOSs attenuate high-fat-diet-induced gut dysbiosis (8) and prevent non-steroidal anti-inflammatory drug-induced small intestinal injury in mice (9) while other studies have shown its biological effects on the peripheral tissues. Enoki et al. (6) reported that orally administered AOSs decreased the edemas of the 12-O-tetradecanoylphorbol-13-acetate-induced ear edema model mice, suggesting that AOSs could translocate from the gastrointestinal tract into the circulating blood and directly reduce inflammatory reactions in peripheral tissues. However, it still remains unclear whether orally administered AOSs permeate across the intestinal epithelium and are absorbed as an intact form.

Caco-2 cells are derived from human colon adenocarcinoma cell line, but this cell line can spontaneously differentiate to express morphological and functional characteristics of mature small intestinal enterocytes, such as microvilli, tight junctions, and some important transporters on the apical membrane (10). Therefore, Caco-2 cells are widely used for *in vitro* studies to investigate the intestinal permeability and their transport mechanisms of drugs and food compounds.

In this study, we aimed to measure the plasma concentrations of AOSs after its oral administration in rats. The blood plasma of the rats orally administered with AOSs was collected and labeled with *p*-aminobenzoic ethyl ester (ABEE). The concentrations of Abi, agarotetraose (Ate), and agarohexaose (Ahe) were measured by liquid chromatography mass spectrometry (LC-MS). In addition, an *in vitro* permeation study was performed to identify the intestinal transport

mechanism of the AOSs across the Caco-2 cell monolayers using different transport inhibitors.

Materials and methods

Chemicals and reagents

Eagle's minimal essential medium (E-MEM), MEM non-essential amino acids (MEM-NEAA) solution, penicillin–streptomycin solution (PS), Hank's balanced salt solution (HBSS), 0.25% w/v trypsin-1 mmol/L ethylenediamine tetraacetic acid·4 Na solution, ethanol, dimethyl sulfoxide (DMSO), sodium chloride, potassium chloride, disodium hydrogen phosphate, potassium dihydrogen phosphate, chloroform, 3-(4,5-dimethylthiazol-2-yl)-2,5-diphenyltetrazolium bromide (MTT), sodium azide, colchicine, cytochalasin B, heparin sodium, and Lucifer yellow CH dilithium salt fluorescent stain (LY) were purchased from FUJIFILM Wako Pure Chemical Corporation (Osaka, Japan). Fetal bovine serum (FBS) was purchased from Merck (Darmstadt, Germany). Acetonitrile was purchased from Nacalai Tesque Inc. (Tokyo, Japan).

Isolation of Abi, Ate, and Ahe

The AOSs were prepared by the acid hydrolysis of agar according to the method described by Enoki et al. (5) with slight modification. In brief, agar was suspended in 0.1 N HCl to 10% (w/v) and heated at 90°C for 30 min. After being cooled to room temperature, powdered activated carbon was added and incubated for 60 min. Powdered activated carbon was filtered and the AOSs solution was freeze dried. The oligosaccharides of different sizes were isolated from the AOSs through size exclusion chromatography using a flash column (15 mm × 170 cm) packed with the Toyopearl HW-40S (Tosoh, Tokyo, Japan) stationary phase at a mobile phase [distilled water (DW)] flow rate of 0.1 ml/min to fractionate the AOSs with different molecular weights (MWs). The obtained each fraction was analyzed with HPLC-refractive index detector (RID-10A, Shimazu, Kyoto, Japan) system. Each fraction was separated on a TSKgel G2500 PWXL (300 × 7.8 mm, 7.0 μm; Showa Denko K.K., Tokyo, Japan). The mobile phase was DW and sent using LC-10AT pump (Shimazu). The fractions were collected and freeze-dried, and then their chemical structures were determined by nuclear magnetic resonance (NMR) spectroscopy to identify Abi, Ate, and Ahe. ^{1}H and ^{13}C NMR spectra (Supplementary Figures 1, 2) were recorded on a Bruker Avance 500 MHz spectrometer in D$_2$O, and chemical shifts of the ^{13}C NMR spectra of Abi and Ate were assigned (Supplementary Table 1).

ABEE derivatization of AOSs

To prepare the standard curve samples of AOSs, the AOSs were labeled with ABEE using an ABEE labeling kit (J-Chemical, Tokyo, Japan) according to the method developed by Yasuno et al. ([11]). The reaction was performed according to the instructions provided by the manufacturer. Briefly, 40 μl of the ABEE reagent solution was added to 10 μl of the solution of AOSs and the mixture was vortexed and incubated at 80°C for 1 h. After cooling to 15–20°C, 200 μl of DW and an equal volume of chloroform were added, and the mixture was then vortexed and centrifuged for 1 min. The upper layer was filtered through a polytetrafluoroethylene membrane (4 mm diameter, 0.45-μm pore size; Membrane Solutions Limited, Plano, TX, USA) and subjected to LC-MS.

Quantification of ABEE-derivatized AOSs by LC-MS

For the HPLC measurements, an LC-20AD pump (Shimadzu) fitted with a DGU-20A 5R degassing unit (Shimadzu) was used. The analytes were injected using a SIL-20AC autosampler (Shimadzu). In addition, a CTO-20AC column oven (Shimadzu) was used, and entire equipment was controlled using a CBM-20A unit (Shimadzu). The samples were separated on a Shim-pack VP-ODS (150 × 2.0 mm, 4.6 μm; Shimadzu) combined with a Shim-pack GVP-ODS guard column (2.0 mm i.d. × 5 mm, 4.6 μm; Shimadzu). The mobile phase consisted of acetic acid (0.1%) in water (A) and acetic acid (0.1%) in acetonitrile (B). The gradient conditions were as follows: 0–30 min, 9%−13% B; 30–45 min, 80% B; 45–60 min, 9% B. The flow rate was 0.2 ml/min. The column oven temperature was set at 60°C, and the autosampler temperature was 10°C.

The detection was performed using an LCMS-2020 (Shimadzu) ESI-MS device. The analytes were identified and quantified by selected ion monitoring in the positive-ion mode. The MS conditions were as follows: interface temperature, 350°C; desolvation line (DL) temperature, 250°C; heat block temperature, 200°C; nebulizer gas flow, 1.5 L/min; drying gas flow, 15 L/min; interface voltage, 4.5 kV; DL voltage, 0 kV.

Animals

Fifteen female Sprague–Dawley rats, aged 7 weeks, were purchased from Charles River Laboratories Japan (Kanagawa, Japan). The rats were acclimatized to standard laboratory conditions (20–25°C, 40%−70% humidity, and 12 h light/dark cycle) for 1 week. All animals had free access to tap water and standard rodent chow (MF; Oriental Yeast Co., Ltd., Tokyo, Japan). All experimental protocols were approved by

the Institutional Animal Care and Use Committee of Shinshu University (Permission No. 020062).
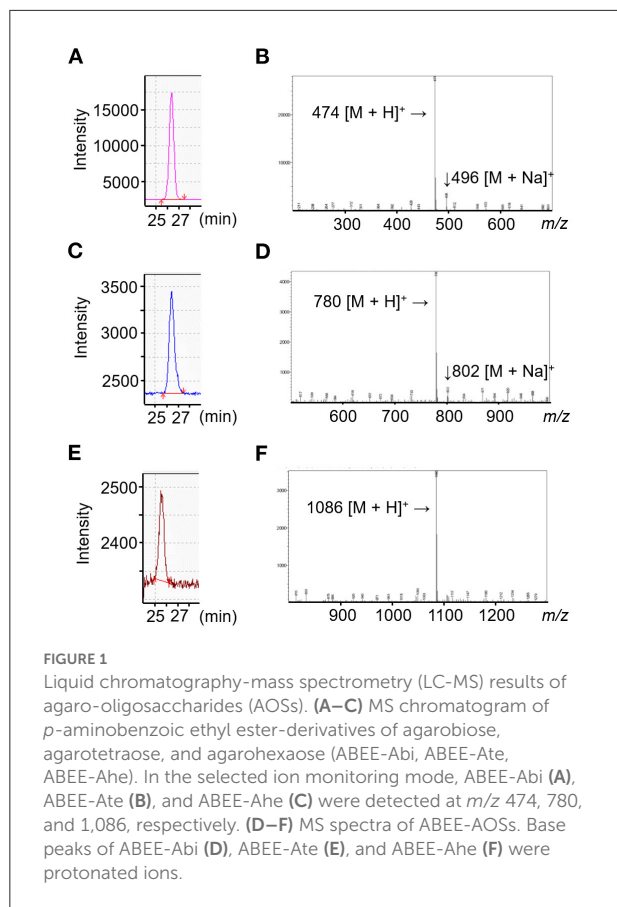
In vivo absorption tests

After a fasting period of 12 h, 2 ml of phosphate-buffered saline (pH 7.4) containing 0%, 10%, or 50% AOSs was orally administered to five rats from each group (220–250 g body weight) using feeding gavages. The AOSs comprised 30.2, 29.1, and 31.6% of Abi, Ate, and Ahe, respectively. Blood (100 μl) was collected before and after 1, 2, 4, 8, and 24 h of oral administration from the tail vein using 10,000 U heparin-coated syringes (1 ml) with a 26G × ½" needle. The blood samples were centrifuged at 1,000 g for 10 min, and the supernatants were collected. Acetonitrile was added to the plasma samples at a final concentration of 60%. The samples were vigorously vortexed and centrifuged at 6,000 g for 5 min; the supernatants were collected and evaporated to dryness. Subsequently, the dried samples were dissolved in 10 μl of DW and subjected to ABEE derivatization before LC-MS analysis. The area under the curve (AUC) of plasma concentration was calculated using the trapezoid formula.

Cell culture for permeation experiments

Caco-2 cells were purchased from DS Pharma (Osaka, Japan). The cells (passage 20–27) were cultured in E-MEM containing 10% (v/v) FBS, 1% (v/v) MEM-NEAA, and 1% (v/v) PS. The cells were incubated at 37°C in an atmosphere of 5% CO_2 under 95% relative humidity. When the cells reached 80–90% confluence, they were passaged at a density of 1.0×10^5 cells onto a 12-well Transwell Permeable Support (0.4-μm pore polyester membrane insert, Corning, NY, USA). The cells were cultured for 19–21 days to obtain a monolayer. The culture medium (0.6 ml in the apical side and 1.5 ml in the basolateral side) was replaced every 1–2 days. The integrity of the Caco-2 cell monolayer was evaluated by measuring transepithelial electrical resistance (TEER) using a Millicell-ERS-2 system (Merck, Darmstadt, Germany). Only cell monolayers with final TEER values above 700 Ω · cm^2, indicative of high barrier integrity, were used for the transport assays.

MTT assay

The cell viability and survivability were determined using an MTT assay. Caco-2 cells were cultured in 96-well microtiter plates at 1×10^5 cells/well in 0.2 ml E-MEM at 37°C. When the cells reached 70% confluence, the culture medium was removed and replaced with different concentrations of Abi or Ahe (0.125, 0.25, 0.5, and 1 mM) in 100 μl of HBSS solution.

FIGURE 1
Liquid chromatography-mass spectrometry (LC-MS) results of agaro-oligosaccharides (AOSs). **(A–C)** MS chromatogram of *p*-aminobenzoic ethyl ester-derivatives of agarobiose, agarotetraose, and agarohexaose (ABEE-Abi, ABEE-Ate, ABEE-Ahe). In the selected ion monitoring mode, ABEE-Abi **(A)**, ABEE-Ate **(B)**, and ABEE-Ahe **(C)** were detected at *m/z* 474, 780, and 1,086, respectively. **(D–F)** MS spectra of ABEE-AOSs. Base peaks of ABEE-Abi **(D)**, ABEE-Ate **(E)**, and ABEE-Ahe **(F)** were protonated ions.

The medium was removed after incubating for 6 h, and 0.15 ml of 0.5 mg/ml MTT solution in HBSS was added to each well. After incubating in the dark for 4 h, the medium was removed, and 0.15 ml of DMSO was added to each well to dissolve formazan crystals, with gentle shaking for 15 min at 37°C. The absorbance was measured at 570 nm using a Nivo Multimode Plate Reader (PerkinElmer, Waltham, MA, USA).

Transepithelial permeation experiment

Caco-2 cells monolayers were preincubated in HBSS for 30 min at 37°C. Subsequently, 0.6 ml of 0.5 mg/ml Abi and Ahe and 1.5 ml of HBSS to the apical and basolateral sides, respectively. After incubation for 0, 1, 2, and 3 h, the supernatant was collected from the basolateral side. To identify the transport mechanisms, Caco-2 cell monolayers were preincubated with sodium azide (1 mM), colchicine (1 mM), or cytochalasin B (5 μg/ml) dissolved in HBSS with 0.1% DMSO for 30 min, followed by the incubation of 0.5 mg/ml Abi and Ahe for 2 h. To remove salt, the collected supernatant was applied to the graphitized carbon solid-phase extraction (GC-SPE) using InertSep GC (200 mg/3 ml) (GL Sciences Inc., Tokyo, Japan),

according to the method described by Ninonuevo et al. (12). The SPE cartridge was first equilibrated with 6 ml of 80% acetonitrile in 0.1% acetic acid (v/v), followed by 3 ml of DW. The basal solution was dissolved in DW to 3 ml and loaded onto the cartridge. The salts were removed by washing with 6 ml of DW, and Abi or Ahe was eluted with 3 ml of 20% acetonitrile. After ABEE derivatization, the collected solution was evaporated to dryness and subjected to LC-MS. The apparent permeability coefficients (*Papp*) were calculated (13) as $Papp = (\mathrm{d}Q/\mathrm{d}t) \times (1/AC_0)$, where $\mathrm{d}Q/\mathrm{d}t$ is the permeation rate (μg/s), A is the area of the monolayer of Caco-2 cells (cm^2), and C_0 is the initial concentration of Abi or Ahe in the apical chamber (μg/ml).

Statistics

Data are presented as the mean ± standard error. The data from the MTT assay were compared using the one-way analysis of variance (ANOVA). The data from the permeation experiment were also compared using one-way ANOVA or the Student's *t*-test. The differences were considered significant at $P < 0.05$. Statcel 4 (OMS Publishing Co., Saitama, Japan) was used for statistical analysis.

Results

Preparation of standard curve of ABEE-derivatized AOSs

The ABEE labeling method was applied to achieve sufficiently high sensitivity for detecting AOSs both *in vivo* and *in vitro*. The ABEE-derivatives of Abi, Ate, and Ahe, denoted as ABEE-Abi, ABEE-Ate, and ABEE-Ahe (Supplementary Figure 3), respectively, were prepared as the standard curve samples. The mass chromatograms and mass spectra obtained for a 5 pmol standard solution of ABEE-Abi, ABEE-Ate, and ABEE-Ahe are illustrated in Figure 1. In the positive-ion mode, the base mass peaks of ABEE-Abi, ABEE-Ate, and ABEE-Ahe were observed at *m/z* 474.3, 780.3, and 1086.3, corresponding to the protonated molecules. The sodium adducts of ABEE-Abi and ABEE-Ate were also detected at *m/z* 496.3 and 802.3, respectively. The linearity of the standard curve ranging from 0.2 to 10 pmol was confirmed for ABEE-Abi, ABEE-Ate, and ABEE-Ahe ($R^2 \geq 0.999$) (Supplementary Figure 4).

AOSs levels in the rat plasma after oral administration

The absorption of AOSs into the bloodstream of rats after oral administration was examined. After administering 1 or 5

FIGURE 2
Plasma concentration−time profiles of Abi **(A)**, Ate **(B)**, and Ahe **(C)** after oral administration of AOSs to rats. Each value represents the mean ± standard error (SE) ($n = 5$).
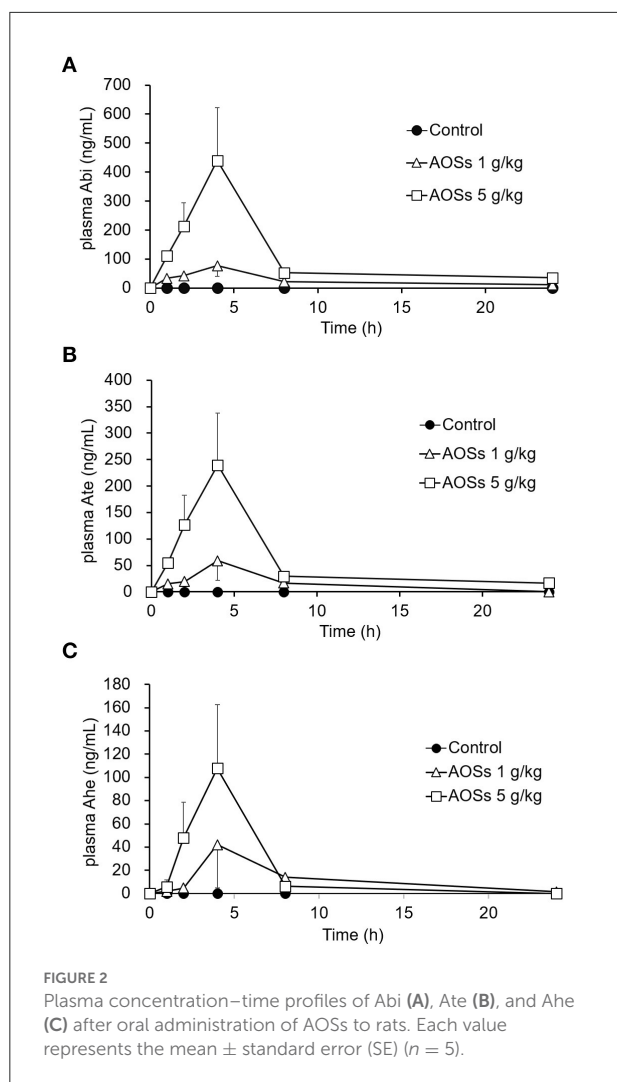
g/kg AOSs, the concentrations of Abi, Ate, and Ahe in the rat plasma increased and reached a maximum value after 4 h (Figure 2). The levels of AOSs detected in the plasma of the rats administered with 5 g/kg AOSs were higher compared with those administered with 1 g/kg AOSs. The AUC and maximum observed plasma concentration (Cmax) values of Abi, Ate, and Ahe in the plasma of the rats administered with 5 g/kg AOSs were higher than those of 1 g/kg AOS (Table 1). The highest AUC and Cmax values were observed in Abi detection, and AOSs with higher MWs were detected to a lower level in the rat plasma. There were no significant differences in Tmax between AOSs with different MWs.

Effects of Abi and Ahe on Caco-2 cell viability

The MTT assay was conducted to evaluate the effects of Abi and Ahe on the Caco-2 cell viability. As shown in Figure 3,

Abi and Ahe did not exhibit cytotoxic effects on Caco-2 cells at concentrations up to 1 mM. Therefore, 0.5 mM of Abi and Ahe was used in the subsequent experiments.

Transepithelial permeation of Abi and Ahe

The Caco-2 cell monolayers cultured on Transwell inserts for 19–21 days were used for the *in vitro* permeation experiments. Both Abi and Ahe permeated the Caco-2 cell monolayers, and the quantity permeated increased linearly with the increasing incubation time (Figure 4). *Papp* (10^{-6} cm/s) of Abi and Ahe was 0.41 ± 0.03 and 0.21 ± 0.01, respectively; the percentage of Abi and Ahe permeated was 0.27 ± 0.02 and $0.14 \pm 0.01\%$/h, respectively.

Analysis of the transepithelial permeation route of Abi and Ahe

The effects of various inhibitors on the transepithelial absorption through Caco-2 cell monolayers were examined to identify the transport routes of Abi and Ahe. We used 1 mM sodium azide and 1 mM colchicine as an electron-transport-chain inhibitor and a transcytosis inhibitor, respectively, to determine whether an energy-dependent pathway is involved. The inhibitors did not have any significant effect on the TEER values or the transport rates of Abi and Ahe (Figures 5A,B). These results suggest that an energy-dependent route was not involved in the transepithelial permeation of AOSs. Next, we used cytochalasin B as a tight junction disruptor to investigate the involvement of the paracellular pathway in the transepithelial permeation of Abi and Ahe. Cytochalasin B increases the paracellular permeability by affecting the tight junction structure through the myosin light chain kinase activation (14). Treatment with 5 μg/ml cytochalasin B significantly decreased the TEER value of the Caco-2 cell monolayers and increased the transepithelial permeability of Abi and Ahe (Figures 5C,D), indicating that Abi and Ahe mainly permeate through the Caco-2 cell monolayers *via* the paracellular pathway.

Correlation between TEER and transepithelial permeation rate of Abi and Ahe
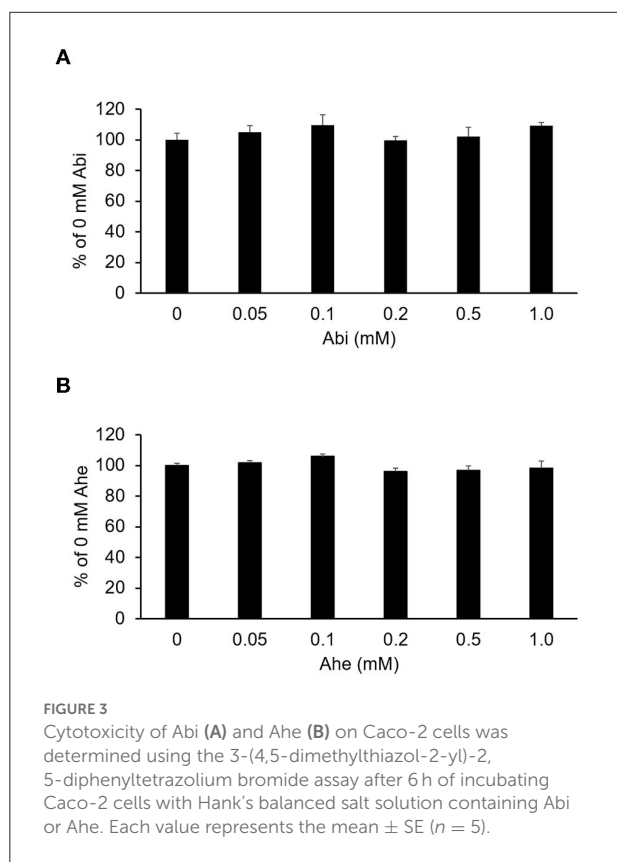
The correlation between TEER and permeation rate was examined to confirm the occurrence of Abi and Ahe transport *via* the paracellular pathway by using the LY fluorescent stain for comparison. Thus, Abi, Ahe, and LY were added to the apical chamber with or without cytochalasin B. The basal chamber

TABLE 1 Pharmacokinetic parameters of orally-administered AOSs in rat plasma.

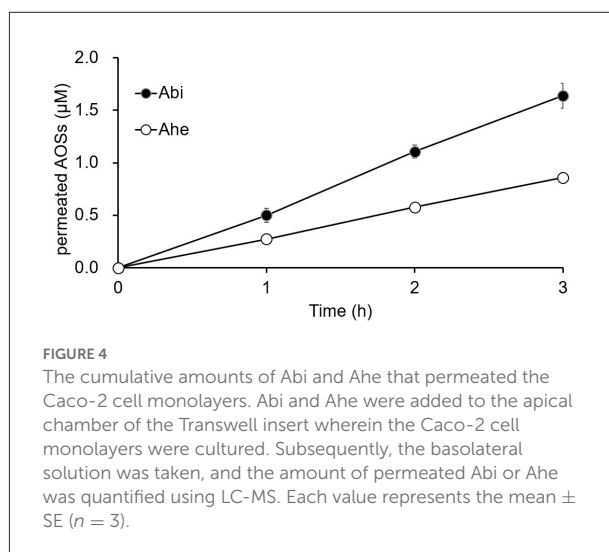| AOSs	1 g/kg			5 g/kg		
	Tmax (h)	Cmax (ng/ml)	AUC (μg·h/ml)	Tmax (h)	Cmax (ng/ml)	AUC (μg·h/ml)
Abi	4	76.4 ± 36.7	0.62 ± 0.18	4	439.8 ± 182.6	2.56 ± 0.81
Ate	4	58.9 ± 37.6	0.39 ± 0.17	4	239.5 ± 98.2	1.39 ± 0.45
Ahe	4	42.1 ± 37.1	0.29 ± 0.27	4	107.8 ± 55.0	0.46 ± 0.25

AOSs, agaro-oligosaccharides; Abi, agarobiose; Ate, agarotetraose; Ahe, agarohexaose; Tmax, time at maximal concentration; Cmax, maximum observed plasma concentration; AUC, area under the curve.

FIGURE 3
Cytotoxicity of Abi (A) and Ahe (B) on Caco-2 cells was determined using the 3-(4,5-dimethylthiazol-2-yl)-2, 5-diphenyltetrazolium bromide assay after 6 h of incubating Caco-2 cells with Hank's balanced salt solution containing Abi or Ahe. Each value represents the mean ± SE ($n = 5$).

FIGURE 4
The cumulative amounts of Abi and Ahe that permeated the Caco-2 cell monolayers. Abi and Ahe were added to the apical chamber of the Transwell insert wherein the Caco-2 cell monolayers were cultured. Subsequently, the basolateral solution was taken, and the amount of permeated Abi or Ahe was quantified using LC-MS. Each value represents the mean ± SE ($n = 3$).

solution was collected, and the TEER was measured every 1 h for 3 h, thereby quantifying Abi, Ahe, and LY in the basal chamber. The TEER and quantified values are plotted as a scatter plot in Figure 6. The Pearson correlation coefficient value of Abi or Ahe was comparable to that of LY (Abi, −0.832; Ahe, −0.814; LY, −0.779).
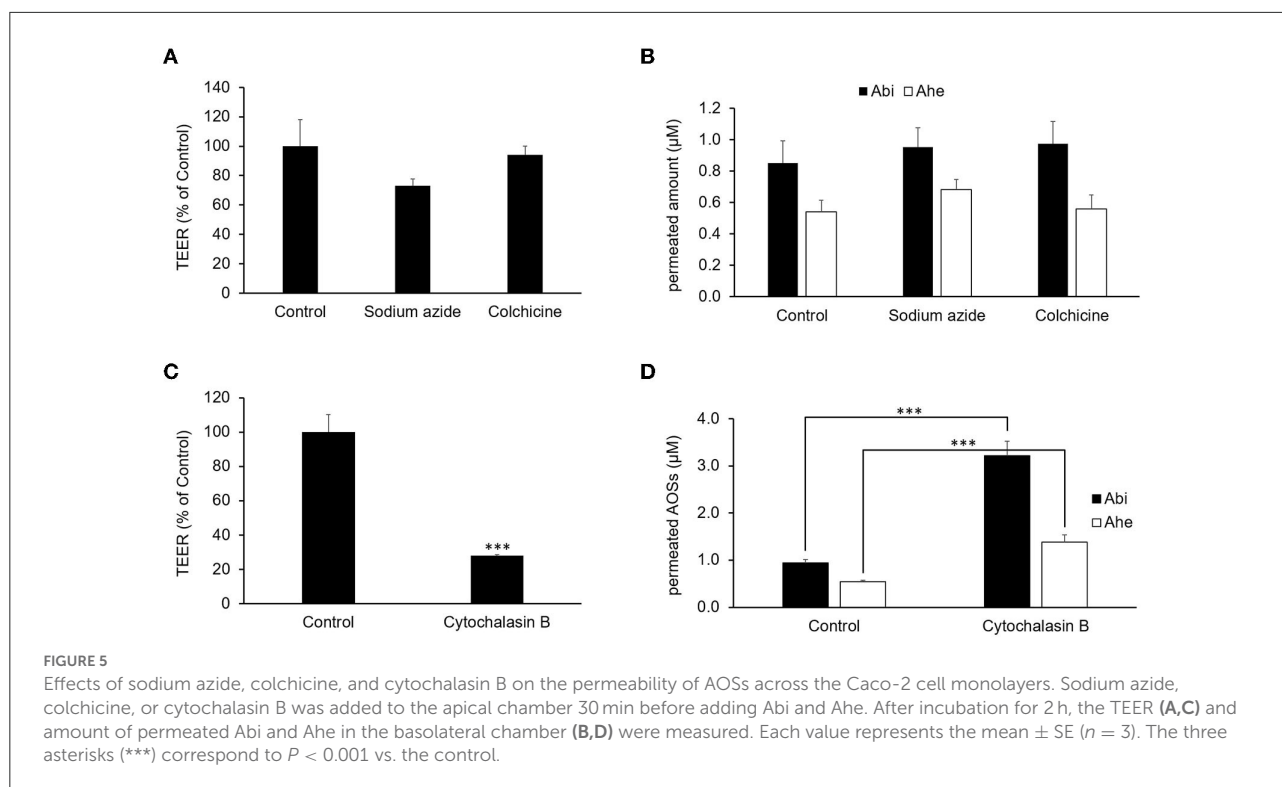
Discussion

This study demonstrated that orally administered AOSs, which are derived from agar, permeated rat plasma. Further, *in vitro* experiments revealed that the AOSs could cross the Caco-2 cell monolayers *via* the paracellular pathway. The plasma samples were derivatized with ABEE to determine the plasma concentration of the orally administered AOSs, which could detect Abi, Ate, and Ahe sensitively and selectively. After orally administering AOSs to the rats, the Abi, Ate, and Ahe concentrations in the plasma were detected. The amount of detected AOSs increased in a time-dependent manner, with an inverse correlation between the plasma detection levels and the MW of the AOSs. *In vivo* pharmacokinetic studies of oligosaccharides or polysaccharides have been conducted previously. For example, in rats, orally administered chitosan oligosaccharides with lower MWs enhance the detection levels (15), which is consistent with our results.

Generally, orally administered carbohydrates are catalyzed to disaccharides by amylase in the saliva and subsequently to monosaccharides by disaccharidases in the brush border membrane. Known transporters of monosaccharides are the sodium–glucose transporter (SGLT) and facilitative glucose transporter (GLUT) families (16, 17). Agarase, the enzyme which hydrolyzes AOSs, is primarily found in marine bacteria,

FIGURE 5
Effects of sodium azide, colchicine, and cytochalasin B on the permeability of AOSs across the Caco-2 cell monolayers. Sodium azide, colchicine, or cytochalasin B was added to the apical chamber 30 min before adding Abi and Ahe. After incubation for 2 h, the TEER **(A,C)** and amount of permeated Abi and Ahe in the basolateral chamber **(B,D)** were measured. Each value represents the mean $\pm$ SE ($n = 3$). The three asterisks (***) correspond to $P < 0.001$ vs. the control.
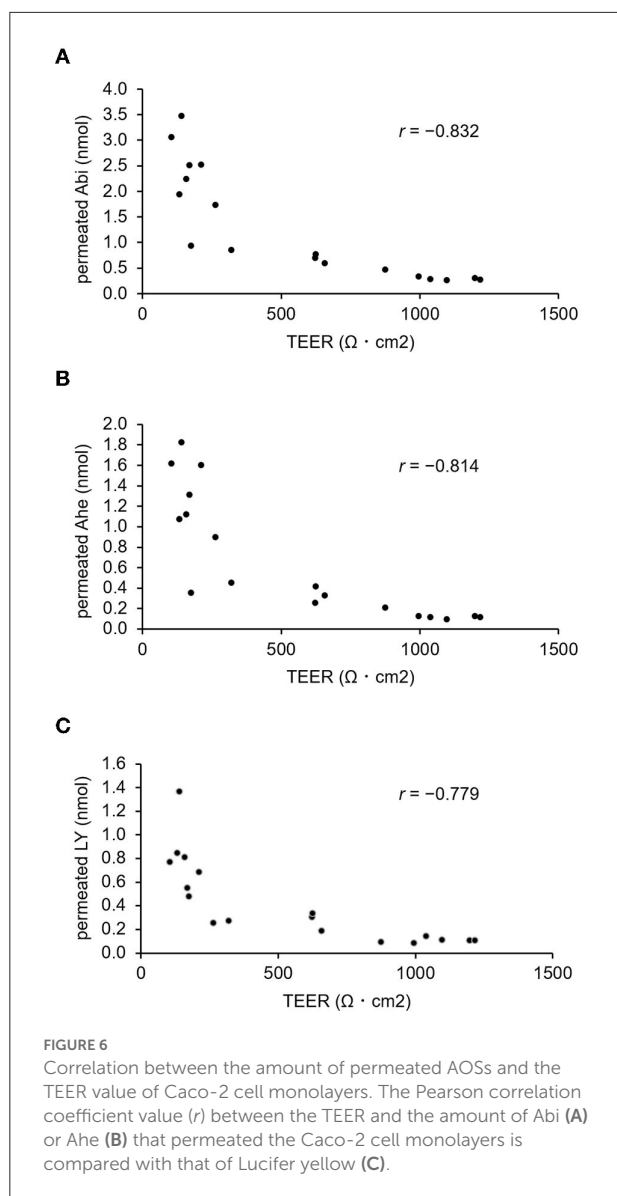
including *Pseudomonas atlantica* (18), *Vibrio* sp. (19), and *Pseudoalteromonas* spp. (20). However, AOSs do not degrade in the mammalian gastrointestinal tracts due to the absence of agarase. This study showed that a metabolic inhibitor (sodium azide) does not inhibit the permeation of Abi or Ahe through Caco-2 cell monolayers. Therefore, AOSs can permeate Caco-2 cell monolayers independently of SGLTs or GLUTs without being degraded by enzymes. In addition, the transport of AOSs was not inhibited by colchicine, which can inhibit intracellular transport (21). Agaro-oligosaccharides were not detected from the cell lysate after the transport experiment (data not shown), suggesting that the transport of AOSs might not proceed *via* the intracellular pathway. In contrast, the permeation of Abi and Ahe was enhanced by treatment with cytochalasin B, a tight junction inhibitor. Furthermore, the Pearson correlation coefficient value of Abi or Ahe is similar to that of LY, a paracellular marker. These results suggest that Abi and Ahe mainly permeated *via* the paracellular pathway.

Paracellular pathway is one of the four distinct transport routes, where tight junctions form an intercellular diffusion barrier between cells, for restricting the transport of macromolecular substances. On the other hand, the paracellular pathway is the preferred route for the transport of hydrophilic substances, including bioactive peptides (22–24) and human milk oligosaccharides (25). The transport mechanism of the peptides GIGLP, RLSFNP, RVPSL have been investigated using

inhibitors of transcytosis and tight junction. The transport rate of these peptides was only modulated after the treatment of tight junction inhibitors. Tight junctions are composed of multiple proteins such as claudin, occludin, zonura occludens-1, and junction adhesion molecule (26). Among tight junction proteins, the structure and function of occludin are most affected by cytochalasin treatment (27), suggesting that permeation of AOSs might be related to decreased occludin. Further investigation using siRNA-mediated knockdown (28) will be needed to elucidate the molecular mechanisms underlying the permeation of AOS.

AOSs exhibit anti-inflammatory activity both *in vitro* and *in vivo*. Enoki et al. (6) demonstrated that oral administration with Abi and Ate to mice resulted in the suppression of nitric oxide (NO) production on stimulated peritoneal macrophages. In this study, mice were treated with 3% AOSs containing water for 3 weeks. Considering the average water consumption of a mouse (30 g mouse, 5 ml water consumption per day), the applied dose meant the intake of 150 mg of AOSs per day, which was consistent with 5.0 g/kg body weight per day of orally administered AOSs. This dosage was same as that used in our study. The AUC and Cmax of AOSs was not significantly detected; however, AOSs might interact with the peritoneal macrophages directly. Future research will be required to assess the absorption rate of orally administered AOSs into human circulation.

FIGURE 6
Correlation between the amount of permeated AOSs and the TEER value of Caco-2 cell monolayers. The Pearson correlation coefficient value (r) between the TEER and the amount of Abi **(A)** or Ahe **(B)** that permeated the Caco-2 cell monolayers is compared with that of Lucifer yellow **(C)**.

The activity of AOSs may depends on the structure of the reducing end. Enoki et al. (5) revealed that neoagarohexaose, which has Gal at the reducing end, exhibited no anti-inflammatory activity, indicating that AnGal at the reducing end is essential for the biological function of AOSs. In addition, there was no relationship between the inhibitory effect on the amount of NO produced and the size of AOSs (including Abi and Ahe) *in vitro*. No information regarding the distribution of AOSs in peripheral tissues is available. Therefore, it could be necessary to determine the distribution of AOSs in different tissues and investigate the degree of bioaccumulation to understand the mechanism underlying the biological effects associated with the molecular size.

Conclusion

The present study evaluated the oral bioavailability and intestinal permeability of AOSs, including Abi, Ate, and Ahe. We demonstrated that orally administered AOSs were detected as their intact forms in the plasma of rats, which were dose-dependently and negatively correlated with MW. Low-MW Abi showed higher permeation compared with high-MW Ahe across Caco-2 cell monolayers, which was consistent with the *in vivo* results. The inhibitors cytochalasin B increased the transport of AOSs across Caco-2 cell monolayers, which implied that the route of transport of AOSs mainly rely on paracellular pathway. These results suggest that orally administered AOSs can be absorbed *via* the gastrointestinal tract into the circulating blood and might exhibit their biological activities in the peripheral tissues such as joints and skin in an intact form. The current findings highlight the potential of the application of AOSs, especially Abi, in the formulation of functional foods or pharmaceuticals.

Data availability statement

The original contributions presented in the study are included in the article/Supplementary material, further inquiries can be directed to the corresponding author.

Ethics statement

The animal study was reviewed and approved by Institutional Animal Care and Use Committee of Shinshu University.

Author contributions

IS, KK, YS, HM, and SK conceived and designed the study. IS, YK, YI, and HM performed the experiments. IS, YI, and HM analyzed the data. IS and HM wrote the manuscript. YS and SK revised the manuscript. All authors read and approved the final version of the manuscript.

Acknowledgments

Conflict of interest

Authors IS and KK are employees of Ina Food Industry Co., Ltd.

The remaining authors declare that the research was conducted in the absence of any commercial or financial relationships that could be construed as a potential conflict of interest.

Publisher's note

All claims expressed in this article are solely those of the authors and do not necessarily represent those of their affiliated organizations, or those of the publisher, the editors and the reviewers. Any product that may be evaluated in this article, or claim that may be made by its manufacturer, is not guaranteed or endorsed by the publisher.

Supplementary material

The Supplementary Material for this article can be found online at: https://www.frontiersin.org/articles/10.3389/fnut.2022.996607/full#supplementary-material

References

1. Araki C, Arai K. Studies on the chemical constitution of agar-agar. XVIII. Isolation of a new crystalline disaccharide by enzymatic hydrolysis of agar-agar. *Bull Chem Soc Japan.* (1956) 29:339–45. doi: 10.1246/bcsj.29.339

2. Chen HM, Zheng L, Yan XJ. The preparation and bioactivity research of agaro-oligosaccharides. *Food Technol Biotechnol.* (2005) 43:29–36.

3. Chen HM, Yan XJ. Antioxidant activities of agaro-oligosaccharides with different degrees of polymerization in cell-based system. *Biochim Biophys Acta.* (2005) 1722:103–11. doi: 10.1016/j.bbagen.2004.11.016

4. Chen H, Yan X, Zhu P, Lin J. Antioxidant activity and hepatoprotective potential of agaro-oligosaccharides *in vitro* and *in vivo. Nutr J.* (2006) 5:31. doi: 10.1186/1475-2891-5-31

5. Enoki T, Okuda S, Kudo Y, Takashima F, Sagawa H, Kato I. Oligosaccharides from agar inhibit pro-inflammatory mediator release by inducing heme oxygenase 1. *Biosci Biotechnol Biochem.* (2010) 74:766–70. doi: 10.1271/bbb.90803

6. Enoki T, Tominaga T, Takashima F, Ohnogi H, Sagawa H, Kato I. Anti-tumor-promoting activities of agaro-oligosaccharides on two-stage mouse skin carcinogenesis. *Biol Pharm Bull.* (2012) 35:1145–9. doi: 10.1248/bpb.b12-00188

7. Higashimura Y, Baba Y, Inoue R, Takagi T, Mizushima K, Ohnogi H, et al. Agaro-oligosaccharides regulate gut microbiota and adipose tissue accumulation in mice. *J Nutr Sci Vitaminol (Tokyo).* (2017) 63:269–76. doi: 10.3177/jnsv.63.269

8. Higashimura Y, Naito Y, Takagi T, Uchiyama K, Mizushima K, Ushiroda C, et al. Protective effect of agaro-oligosaccharides on gut dysbiosis and colon tumorigenesis in high-fat diet-fed mice. *Am J Physiol Gastrointest Liver Physiol.* (2016) 310:G367–75. doi: 10.1152/ajpgi.00324.2015

9. Higashimura Y, Naito Y, Takagi T, Tanimura Y, Mizushima K, Harusato A, et al. Preventive effect of agaro-oligosaccharides on non-steroidal anti-inflammatory drug-induced small intestinal injury in mice. *J Gastroenterol Hepatol.* (2014) 29:310–7. doi: 10.1111/jgh.12373

10. Iftikhar M, Iftikhar A, Zhang H, Gong L, Wang J. Transport, metabolism and remedial potential of functional food extracts (FFEs) in Caco-2 cells monolayer: a review. *Food Res Int.* (2020) 136:109240. doi: 10.1016/j.foodres.2020.109240

11. Yasuno S, Kokubo K, Kamei M. New method for determining the sugar composition of glycoproteins, glycolipids, and oligosaccharides by high-performance liquid chromatography. *Biosci Biotechnol Biochem.* (1999) 63:1353–9. doi: 10.1271/bbb.63.1353

12. Ninonuevo MR, Park Y, Yin H, Zhang J, Ward RE, Clowers BH, et al. A strategy for annotating the human milk glycome. *J Agric Food Chem.* (2006) 54:7471–80. doi: 10.1021/jf0615810

13. Artursson P, Palm K, Luthman K. Caco-2 monolayers in experimental and theoretical predictions of drug transport. *Adv Drug Deliv Rev.* (1996) 22:67–84. doi: 10.1016/S0169-409X(96)00415-2

14. Ma TY, Hoa NT, Tran DD, Bui V, Pedram A, Mills S, et al. Cytochalasin B modulation of Caco-2 tight junction barrier: role of myosin light chain kinase. *Am J Physiol Gastrointest Liver Physiol.* (2000) 279:G875–85. doi: 10.1152/ajpgi.2000.279.5.G875

15. Chae SY, Jang MK, Nah JW. Influence of molecular weight on oral absorption of water soluble chitosans. *J Controll Release.* (2005) 102:383–94. doi: 10.1016/j.jconrel.2004.10.012

16. Drozdowski LA, Thomson AB. Intestinal sugar transport. *World J Gastroenterol.* (2006) 12:1657–70. doi: 10.3748/wjg.v12.i11.1657

17. Cura AJ, Carruthers A. Role of monosaccharide transport proteins in carbohydrate assimilation, distribution, metabolism, and homeostasis. *Compr Physiol.* (2012) 2:863–914. doi: 10.1002/cphy.c110024

18. Morrice LM, McLean MW, Long WF, Williamson FB. β-agarases I and II from *Pseudomonas atlantica.* Substrate specificities. *Eur J Biochem.* (1983) 137:149–54. doi: 10.1111/j.1432-1033.1983.tb07808.x

19. Sugano Y, Matsumoto T, Kodama H, Noma M. Cloning and sequencing of agaA, a unique agarase 0107 gene from a marine bacterium, Vibrio sp. strain JT0107. *Appl Environ Microbiol.* (1993) 59:3750–6. doi: 10.1128/aem.59.11.3750-3756.1993

20. Oh YH, Jung C, Lee J. Isolation and characterization of a novel agarase-producing *Pseudoalteromonas* spp. bacterium from the guts of spiny turban shells. *J Microbiol Biotechnol.* (2011) 21:818–21. doi: 10.4014/jmb.1012.12027

21. Andreu JM, Timasheff SN. Tubulin bound to colchicine forms polymers different from microtubules. *Proc Natl Acad Sci USA.* (1982) 79:6753–6. doi: 10.1073/pnas.79.22.6753

22. Ding L, Zhang Y, Jiang Y, Wang L, Liu B, Liu J. Transport of egg white ACE-inhibitory peptide, Gln-Ile-Gly-Leu-Phe, in human intestinal Caco-2 cell monolayers with cytoprotective effect. *J Agric Food Chem.* (2014) 62:3177–82. doi: 10.1021/jf405639w

23. Guo Y, Gan J, Zhu Q, Zeng X, Sun Y, Wu Z, et al. Transepithelial transport of milk-derived angiotensin I-converting enzyme inhibitory peptide with the RLSFNP sequence. *J Sci Food Agric.* (2018) 98:976–83. doi: 10.1002/jsfa.8545

24. Ding L, Wang L, Zhang Y, Liu J. Transport of antihypertensive peptide RVPSL, ovotransferrin 328-332, in human intestinal Caco-2 cell monolayers. *J Agric Food Chem.* (2015) 63:8143–50. doi: 10.1021/acs.jafc.5b01824

25. Gnoth MJ, Rudloff S, Kunz C, Kinne RK. Investigations of the *in vitro* transport of human milk oligosaccharides by a Caco-2 monolayer using a novel high performance liquid chromatography-mass spectrometry technique. *J Biol Chem.* (2001) 276:34363–70. doi: 10.1074/jbc.M104805200

26. Balda MS, Matter K. Transmembrane proteins of tight junctions. *Semin Cell Dev Biol.* (2000) 11:281–9. doi: 10.1006/scdb.2000.0177

27. Madara JL, Barenberg D, Carlson S. Effects of cytochalasin D on occluding junctions of intestinal absorptive cells: further evidence that the cytoskeleton may influence paracellular permeability and junctional charge selectivity. *J Cell Biol.* (1986) 102:2125–36. doi: 10.1083/jcb.102.6.2125

28. Costa Verdera H, Gitz-Francois JJ, Schiffelers RM, Vader P. Cellular uptake of extracellular vesicles is mediated by clathrin-independent endocytosis and macropinocytosis. *J Control Release.* (2017) 266:100–8. doi: 10.1016/j.jconrel.2017.09.019